

Characteristics of gravity waves generated in a convective and a non-convective environment revealed from hourly radiosonde observation under CPEA-II campaign

S. K. Dhaka¹, R. Bhatnagar^{1,2}, Y. Shibagaki³, H. Hashiguchi⁴, S. Fukao⁴, T. Kozi⁵, and V. Panwar^{1,2}

¹Radio and Atmospheric Physics Lab, Department of Physics, Rajdhani College, University of Delhi, Delhi, India

²Department of Physics and Astrophysics, University of Delhi, India

³Faculty of Information and Communication Engineering, Osaka Electro-Communication University, Japan

⁴Research Institute for Sustainable Humanosphere, Kyoto University, Japan

⁵Interdisciplinary Faculty of Science and Engineering, Shimane University, Japan

Received: 29 May 2010 – Revised: 5 November 2011 – Accepted: 8 November 2011 – Published: 16 December 2011

Abstract. Analyses of hourly radiosonde data of temperature, wind, and relative humidity during four days (two with convection and two with no convection) as a part of an intensive observation period in CPEA-2 campaign over Koto Tabang (100.32° E, 0.20° S), Indonesia, are presented. Characteristics of gravity waves in terms of dominant wave frequencies at different heights and their vertical wavelengths are shown in the lower stratosphere during a convective and non-convective period. Gravity waves with periods ~ 10 h and ~ 4 – 5 h were found dominant near tropopause (a region of high stability) on all days of observation. Vertical propagation of gravity waves were seen modified near heights of the three identified strong wind shears (at ~ 16 , 20, and 25 km heights) due to wave-mean flow interaction. Between 17 and 21 km heights, meridional wind fluctuations dominated over zonal wind, whereas from 22 to 30 km heights, wave fluctuations with periods ~ 3 – 5 h and ~ 8 – 10 h in zonal wind and temperature were highly associated, suggesting zonal orientation of wave propagation. Gravity waves from tropopause region to 30 km heights were analyzed. In general, vertical wavelength of 2–5 km dominated in all the mean-removed (\sim weekly mean) wind and temperature hourly profiles. Computed vertical wavelength spectra are similar, in most of the cases, to the source spectra (1–16 km height) except that of zonal wind spectra, which is broad during active convection. Interestingly, during and after convection, gravity waves with short vertical wavelength (~ 2 km) and short period (~ 2 – 3 h) emerged, which were confined in the close vicinity of tropopause, and were not identified on non-convective days, suggesting convection to

be the source for them. Some wave features near strong wind shear (at 25 km height) were also observed with short vertical wavelengths in both convective and non-convective days, suggesting wind shear to be the sole cause of generation and seemingly not associated with deep convection below. A drop in the temperature up to ~ 4 – 5 K (after removal of diurnal component) was observed at ~ 16 km height near a strong wind shear (~ 45 – 55 m s⁻¹ km⁻¹) during active period of convection.

Keywords. Meteorology and atmospheric dynamics (Convective processes)

1 Introduction

The active cumulus convection in the equatorial region is the source of many unique atmospheric processes that couple the Earth's atmosphere from bottom to top and from equator to poles. Owing to the minimal Coriolis effect present in the equatorial region, a wide range of atmospheric waves in time and space are generated, which propagate upward and interact with the background mean flow. The Indonesian region, located in the equatorial belt, is known for its most active and strong convective activities where the vertical coupling takes place most conspicuously. The diurnal strong localized convection activities modulate the ambient atmospheric conditions in the troposphere and lower stratosphere (UTLS) region. Short period gravity waves (with a period range of a few minutes to a few hours) had been reported directly above convection using radar data (Dhaka et al., 2005, 2006, 2007b). However, radar observations are mostly limited up to 20 km height owing to the instrument capability; therefore,



Correspondence to: S. K. Dhaka
(skdhaka@yahoo.com)

data above 20 km are not explored much at a fine time and height resolution to provide wave characteristics.

Fritts and Alexander (2003) had reviewed the status of the gravity waves (GWs) regarding their sources and characteristic features in the atmosphere by citing several studies including those of simulations and observations (Lane et al., 2001; Vincent and Alexander, 2000). There are several suggested mechanisms to generate GWs such as convection, mountains, jet streams, cyclones, etc. Once they are generated, their vertical propagation depends on the basic state of wind. GWs can be filtered, dissipated or amplified, depending upon the background conditions. Fritts and Alexander (2003) emphasized in their study that there is little understanding of the characteristics of the GWs spectrum and its behavior with altitude due to variability imposed by sources, mean wind and low frequency motions. Also, global climatology of gravity waves and their effects, including the processes and interaction that constrain wave amplitudes, etc. are not well understood. Some efforts along these lines have been made by Lane et al. (2001, and references therein) and Ratnam et al. (2004).

Therefore, an understanding of the structure and dynamics of the atmosphere and its variability due to energy and momentum transport by short period internal GWs is essential. Some efforts have been made in the past to investigate such relationships (Alexander et al., 1995; Abraham et al., 1998; Horinouchi et al., 2002; Chun et al., 2004; Dhaka et al., 2005, 2006). Ratnam et al. (2004) have shown the variation in potential energy in the stratosphere, showing its larger values in the tropics in association with low OLR. Nonetheless, the South-East Asian region is still unexplored regarding detailed investigation of sources and characteristic features of GWs in the lower stratosphere. Temperature of the tropopause region is also unexplored at a very fine time and vertical scale during a passage of convection. These aspects will be examined in this study.

Recently, Alexander et al. (2008) studied tidal components over the Indonesian/Darwin region using radiosonde campaigns data (DAWEX – 2001, TWPICE – 2006, CPEA – November 2002, CPEA-I – April–May 2004, and CPEA-II – November–December 2005) over several stations. Using radar and radiosonde data, they emphasized that tidal components contribute significantly to the variation of wind and temperature perturbations in the troposphere and stratosphere. In addition, they mentioned that amplitude of diurnal tide did not depend on the strength of tropospheric convection at Koto Tabang (100.32° E, 0.20° S); rather, they are related to QBO and associated wind shear at stratosphere. Both migrating and non-migrating tidal components were observed with a tentative interaction between non-migrating tides and QBO, owing to its low phase speed.

Some studies in the past have been performed on the characteristics of GWs over Indonesia (e.g. Tsuda et al., 1994). They focused on wave systems with wave periods 3–5 days, having horizontal wavelengths 500–800 km in the

troposphere. These waves were found to be associated with convection in the troposphere. Wave motions with periods of 3–5 days in the stratosphere were associated with longer horizontal wavelengths (~ 2000 km). Recently, well coordinated observational campaigns were conducted under Coupling Processes in the Equatorial Atmosphere (CPEA) program over Indonesia from September 2001 to March 2007 (Fukao, 2006). In these campaigns, spatial and temporal variability of various atmospheric waves and dynamical and electro-dynamical coupling processes in the equatorial atmosphere were investigated in the wide altitude range from troposphere to the thermosphere/ionosphere. One of the objectives of the CPEA campaign was to study the atmospheric dynamics using a suite of instruments to gain a better understanding of equatorial convection and associated wave systems. Growth of the convection systems were measured using temperature and wind data obtained from UHF radar, X-band radar, radiosonde, satellite (MTSAT – 1R), and EAR data (Shibagaki et al., 2006a, b; Dhaka et al., 2005, 2006). Because the altitude coverage of individual instruments is limited, the atmosphere up to about 35 km height was covered by operating all the instruments simultaneously. Under the CPEA program, two extensive observation campaigns were conducted, which together have provided numerous new results on the vertical coupling of equatorial atmosphere.

The first CPEA campaign was conducted April–May 2004 (summer season) and the second campaign was held November–December 2005 (winter season). In the CPEA-I campaign, study of GWs (Ratnam et al., 2006), Kelvin waves (Tsuda et al., 2006; Dhaka et al., 2007a), and local convection induced gravity waves (Dhaka et al., 2006; Alexander et al., 2006) were investigated at length using mainly Equatorial Atmosphere Radar (EAR) and radiosonde data. These waves with different horizontal wavelengths are reported to be originated from organized and local convection on different scales in the Indonesian region. Sometimes organized convections were seen stretched from the Indian Ocean to the Indonesian region in the form of super cloud clusters moving eastward. These eastward-moving clusters are often seen associated with intra-seasonal oscillations commonly known as Madden-Julian Oscillations (Shibagaki et al., 2006b).

In the CPEA-II campaign (18 November 2005 to 23 December 2005), various observations were conducted in the Indonesian equatorial region with the main facility of EAR at Koto Tabang. Radiosondes were also launched on an hourly basis on certain days during the campaign period that provided temperature and horizontal wind components up to 30–35 km in height.

In this study, we made use of CPEA-II campaign data obtained from hourly radiosonde flights launched on 30 November and 9 December 2005 (convection days), and 6 December and 18 December 2005 (no convection days). Using such a unique data set, wave motions at a fine temporal resolution (~ 2 h wave period) in the UTLS region and above (~ 30 km height) on convection days could be studied.

Because such a fine temporal resolution (1 h) of radiosonde data could not be obtained in CPEA-I campaign and elsewhere, it assumes a lot of significance regarding its provision of information on temperature, humidity, and wind variability in the convective environment. We analyzed this data set to identify the forcing scale in the vertical direction in order to determine wavelength and dominant wave frequencies at different altitudes, especially above 16 km heights. Section 2 includes details of the data used. Main results and discussions are described in Sect. 3. Concluding remarks and summary are given in Sect. 4.

2 Data used

Wind, temperature and humidity were observed as part of a well-coordinated intensive observation period (IOP) under CPEA-II campaign at Koto Tabang (100.32° E, 0.20° S), West Sumatra, Indonesia. Observations were taken from 18 November 2005 to 23 December 2005 using hourly radiosonde launchings on certain days. We present four days of observations consisting of two with convection (30 November and 9 December 2005) and two with no convection days (6 December and 18 December 2005). These two convective events were fully observed by hourly launching of radiosonde. Although convective events occurred on other days as well, those were not completely covered by radiosonde observations. About 19 radiosondes were launched on each day. Convection events occurred in the late afternoon and evening hours on 30 November 2005 and 9 December 2005 with the following average daily rainfall rate: $\sim 0.2 \text{ mm h}^{-1}$ on 30 November 2005 and $\sim 2.5 \text{ mm h}^{-1}$ on 9 December 2005, respectively.

We focused on the characteristics of short period GWs with time periods of 2–10 h in the UTLS region. Data was passed through a high pass filter (Schodel and Munk, 1972) with cutoff at 12 h to remove the diurnal cycle in temperature and wind components. This was performed to make the appropriate use of hourly radiosonde observations and also to measure changes in the thermal structure of the tropopause caused by convection. Power spectrum using maximum entropy method (MEM) was applied to determine the dominant frequencies and wavelength (Barrodale and Erikson, 1980). Results obtained using MEM were also compared with the FFT technique; they are in good agreement. We comprehensively analyzed two convective and two non-convective days' data, enabling us to compare the characteristics of short period GWs.

Radiosondes (Vaisala RS-92) were launched every hour (13:00 to 24:00 LST; 00:00 to 07:00 LST). Data was obtained from 1 to 30 km height at a high vertical resolution ($\sim 10 \text{ m}$), further smoothed out at an interval of 100 m for the present study. A capacitive wire type temperature sensor used in radiosonde covered a range from -90°C to -60°C and with a resolution of 0.1°C and accuracy of 0.3°C . The

silicon type pressure sensor covered a range from 1080 hPa to 3 hPa vertically with 0.1 hPa resolution and 0.5 hPa accuracy. The humidity sensor of thin-film capacitor type in radiosonde provided humidity data with 1 % RH resolution and 5 % RH accuracy.

High temporal ($\sim 1 \text{ h}$) and spatial resolution ($0.05^\circ \times 0.05^\circ$) satellite brightness temperature data, provided by Multifunctional Transport Satellite (MTSAT – 1R), were used to determine the cloud top temperature during observation period. Satellite data were obtained from Japan Meteorological Agency (JMA) through Kochi University, Japan. Equatorial Atmosphere Radar (EAR) also operated continuously during hourly radiosonde launching. Observations were made for vertical wind near tropopause region to examine the effect of enhanced humidity and of subsequent large fluctuations in temperature during convection in the upper tropospheric region. The accuracy of the vertical wind measurement is 0.1 m s^{-1} with height resolution of 150 m. In addition, we made use of UHF radar reflectivity to determine the depth and intensity of convection in the troposphere region near the EAR site. Using satellite and UHF radar data, one can infer the cloud top temperature and vertical depth of the convection system. Observations regarding the horizontal movement of convective clouds at a particular height were taken using X-Band radar reflectivity data, which are important to decipher the temporal evolution of the convective system. The X-band radar reflectivity obtained during observation period is shown in Sect. 3.1.

3 Results and discussions

3.1 Evolution and dissipation of convection observed using satellite and X-band radar

Figure 1 (upper panels; top left and middle) shows satellite-derived cloud top brightness temperature data obtained on 30 November 2005 and 9 December 2005 at the time of active convection. Deep clouds observed during convective system in the evening ($\sim 16:00\text{--}20:00 \text{ LST}$), dissipate within a few hours from termination of convection.

Figure 1c shows no sign of convective cloud on 6 December 2005. Scale of color code is shown alongside; the range of cloud top temperature from -60°C to -70°C corresponds to deep clouds over the radar area. The ambient atmospheric condition in the lower troposphere was being monitored using X-band radar. Figure 1d–f shows the temporal evolution of convective events (on 6 December 2005 there was no convection) within a radius of 60 km on 30 November 2005, 9 December 2005, and 6 December 2005 over a period of 24 h. Variation in radar reflectivity (dBZ) denote the convection strength at an altitude of 2.1 km. Negative (positive) values on the y-axis denotes west (east) side of the radar.

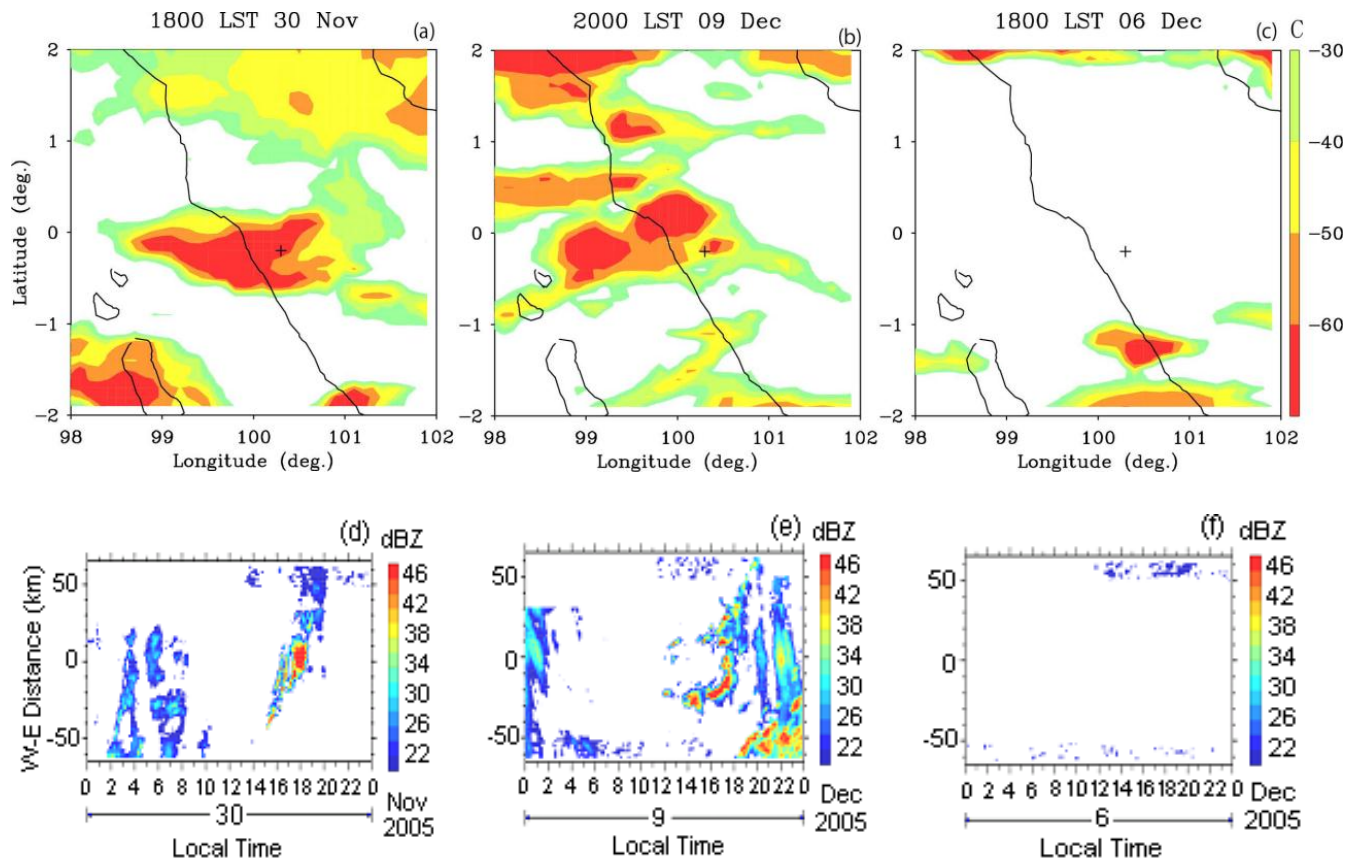


Fig. 1. Satellite (MTSAT – 1R) derived cloud top temperature. The panels are constructed within 2° N to 2° S latitude and 98° E to 102° E longitude covering EAR site. “+” sign denotes location of the radar. Color scale denotes the different temperature ranges. Upper panels show temperature at (a) 18:00 LST on 30 November, (b) 20:00 LST on 9 December, and (c) 18:00 LST on 6 December, while lower panels (d) to (f) show X-band radar reflectivity on 30 November 2005, 9 December 2005, and 6 December 2005, respectively. Data are not shown on 18 December 2005 as no convection was observed and the satellite temperature and X-band reflectivity obtained were similar to (c) and (f), respectively.

Convection appeared at around 50 km in the west of the radar site at 15:00 h on 30 November 2005. There is a possibility of advection of the convective system over the radar area as the convective system moved eastward with time. Eastward movement is in association with wind in the lower troposphere. Strong convection was observed at 17:00–18:00 LST with high radar reflectivity (~ 40 – 46 dBZ). Convection dissipated within 4–5 h in the east of the radar. Note that the two sets of independent observations (cloud top brightness temperature from MTSAT-1R satellite and X-Band radar reflectivity) show occurrence of convection at the same time, confirming the accuracy of instruments.

Similar features of convection evolution and dissipation were observed on 9 December 2005 as seen in Fig. 1b. A strong convective event occurred in the late evening ($\sim 20:00$ LST), which lasted for a longer period (up to 03:00 h on 10 December 2005) in comparison to the 30 November 2005 event. Direction of low level convection was not as clear as seen on 30 November 2005; rather, it appeared in all directions.

Thermal structure in the upper troposphere changed substantially. Considerable cooling and change in wind speed and direction are shown later in Sect. 3.3 (Fig. 5).

3.2 Horizontal wind, temperature and ambient atmospheric conditions

Vertical profiles of wind, temperature, and wind shear are shown in Fig. 2. These profiles provide the ambient atmospheric conditions in the troposphere and lower stratosphere. Temperature and wind anomalies are shown in the supplement (Fig. A1 and A2) on 9 December 2005 as a sample graph to show the changes in temperature and wind field before, during, and after the convection. Figure 2 shows average profiles of temperature, horizontal wind (zonal and meridional wind components), and wind shear on 4 different days: two with convective (30 November 2005 and 9 December 2005) and two non-convective (dry) days (6 December 2005 and 18 December 2005). The average profiles were computed using 17 profiles for 6 December and

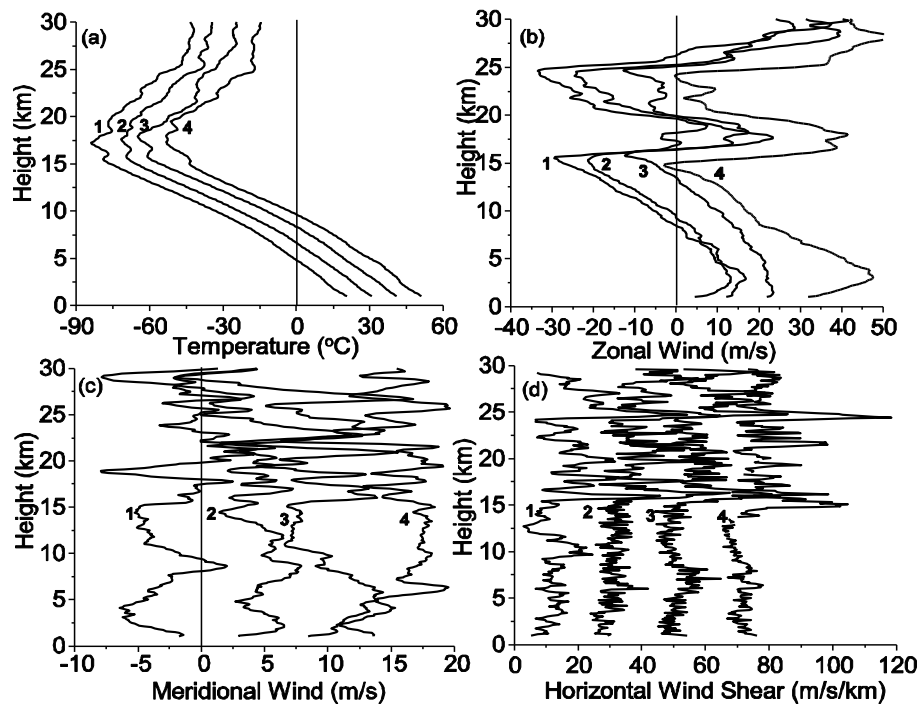


Fig. 2. Vertical profiles of (a) temperature ($^{\circ}\text{C}$), (b) zonal wind, (c) meridional wind, (d) and horizontal wind shear on four different observation days (numerals 1, 2, 3, and 4 on profiles denote 30 November, 6 December, 9 December, and 18 December 2005, respectively). A constant number (10 in panels a and b, 5 in panel c, and 20 in panel d) is added to avoid overlapping in all the panels. The average profiles were computed using 17 profiles for 6 December, and 19 profiles for the other three days.

Table 1. Details of wind shear on all four days of observations.

Date	Wind shear 1		Wind shear 2		Wind shear 3	
	Height (km)	Value ($\text{m s}^{-1} \text{ km}^{-1}$)	Height (km)	Value ($\text{m s}^{-1} \text{ km}^{-1}$)	Height (km)	Value ($\text{m s}^{-1} \text{ km}^{-1}$)
30 Nov 2005 (CONV)	16.0	45.7	18.0	32.0	24.7	54.0
9 Dec 2005 (CONV)	16.2	58.6	19.3	28.2	24.8	46.0
6 Dec 2005 (NOCONV)	16.3	47.7	19.7	42.0	24.6	44.6
18 Dec 2005 (NOCONV)	15.1	44.8	19.3	30.0	24.4	58.0

19 profiles for the other three days. Profiles in Fig. 2 are shifted rightward to avoid overlapping by adding constant number(s) (mentioned in figure caption). Mean profiles of temperature (T) and wind showed similar features over a time interval of about 20 days (from 30 November–18 December 2005). Cold point tropopause (CPT) temperature decreased by $\sim 3^{\circ}\text{C}$ on both convection days.

Easterly wind (U) prevailed in the middle and upper troposphere, showing maximum speed near 16 km height ($\sim -30 \text{ m s}^{-1}$). At higher heights around 25 km, strong easterly wind ($\sim 35 \text{ m s}^{-1}$) prevailed (Fig. 2b). Over a period of about 20 days (30 November–18 December 2005), maximum wind speed below tropopause (at $\sim 14.8 \text{ km}$ to 15.8 km height) increased from -30 m s^{-1} to -33 m s^{-1} . In contrast,

wind speed near the 25 km height decreased from -35 m s^{-1} to -30.4 m s^{-1} .

Figure 2c shows meridional mean wind (V) profiles in the height region of 1–30 km. Below tropopause, V wind turned from southward to northward (-4 m s^{-1} to 5 m s^{-1}) during 30 November–18 December 2005. Intensive wind speed was observed in the troposphere. It maximized at ~ 20 – 22 km and 27 – 28 km heights. Thus, the height region of 15–30 km was dominated by three strong wind shears located near 16 km (referred to as WS1), 20 km (referred to as WS2), and 25 km (referred to as WS3) heights, respectively, as shown in Fig. 2d. Near 16 km height, maximum wind shear ($\sim 58.6 \text{ m s}^{-1} \text{ km}^{-1}$) was observed on 9 December 2005 – a convection day. Near 25 km height, wind shear

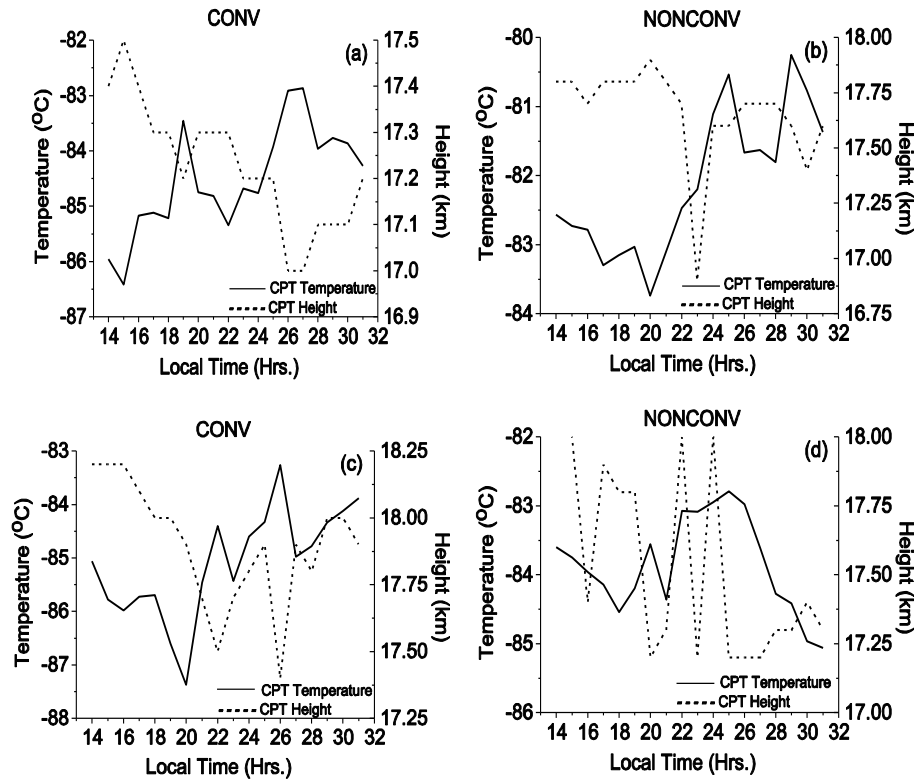


Fig. 3. (a)–(d) represents hourly variation of Cold Point Tropopause temperature (solid line) and height (dotted line) for (a) 30 November 2005, (b) 6 December 2005, (c) 9 December 2005 and (d) 18 December 2005, respectively. On time scale, one hour is added to compensate the timing of the radiosonde to reach the level of tropopause.

varied on four different observation days, showing no relation with the convection occurrence below that height. Details of three wind shears on each day are provided in the Table 1.

To examine the hourly variations of CPT and its corresponding height, we have shown all four cases in Fig. 3. Wave-like structure with periods 3–5 h and ~ 10 h in CPT temperature, along with similar periods in the tropopause height, is seen. On convection days, there is a marked tendency of increasing (decreasing) CPT height (CPT temperature). The CPT temperature lowered on both the convective days (~ -85 °C) in comparison to non-convective days (~ -82 °C) with CPT height at ~ 17.3 km. Such a decrease in temperature is caused by the convective environment in the upper troposphere.

Generally, in the late evenings on all days, CPT temperature increased with a decrease in CPT height. Wave-like fluctuations are apparent in the hourly temperature and height. Mean height of the CPT remains at about 17.3 km. However, during active convection, CPT height drops but it recovers its mean height after termination of convection. Such phenomena leads to the generation of wave patterns at ~ 15 –17 km heights. By carefully examining the lowest temperature near 15–17 km heights, double tropopause was observed (showing

almost similar temperature). Heights of the two tropopause levels seems to merge with time (shown later in Sect. 3.4, Fig. 7d).

3.3 Atmospheric stability condition

Figure 4 shows averaged vertical profiles of Richardson number (Ri) before and during convection occurrence on 30 November (Fig. 4a and b) and 9 December 2005 (Fig. 4c and d). Vertical line drawn on x-axis denotes the critical limit of Ri for setting up of the turbulence. Ri profiles before and during the convection showed a variation in the troposphere. During convection, values less than 0.25 (critical value for setting up the turbulence or instability) are more frequent in comparison to those computed before the convection occurrence in the upper troposphere. We have also checked the subsequent profiles to examine the gradual change in atmospheric stability in the tropospheric region during formation of convection, its maturation and dissipation. It is noticed that middle and upper troposphere, during convection, do not show stable conditions (as confirmed by Ri values, which lie near 0.25 line and at some of the heights below tropopause, Ri is negative – near WS1).

The atmospheric conditions, in general, in the upper troposphere are more stable on non-convection days (6 December

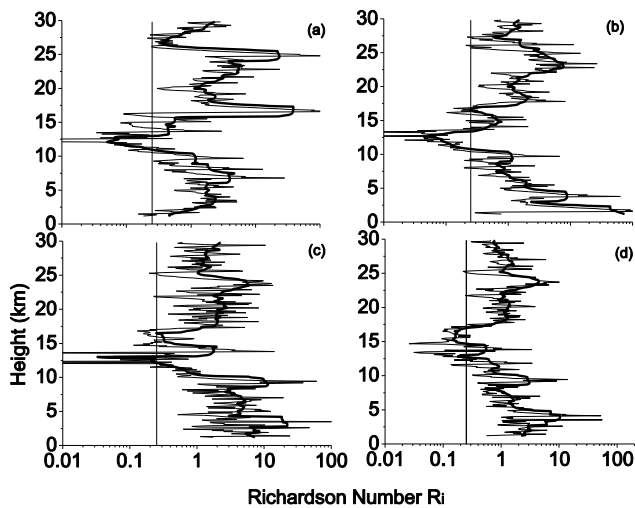


Fig. 4. Richardson number profiles for 30 November 2005 (a) before and (b) during convection (top panel), and for 9 December 2005 (c) before and (d) during convection (bottom panel). Both the panels represent convective days' observation. Note that a vertical line at 0.25 on x-axis denotes demarcation between states of turbulence and stable atmosphere. Dark line represents average profile using running mean of 1.5 km.

and 18 December 2005) than those observed on convective days. However, very close to wind shear region (~ 16 km) there are thin layers that have less Ri values, showing lesser stability. Non-convective days have been selected to examine the difference between the convective and non-convective environment. Near the strong wind shears at higher heights, for instance at ~ 20 km (near WS2), Ri drops to the critical limit (0.25); this level seems affected with the convection occurrence (enhanced perturbations in time series of temperature and wind up to 19–20 km heights – not shown here). However, near the 25 km height – a region of WS3 – Ri shows a drop to the critical value of 0.25, which does not seem to have a close association with convective system but rather appears generated due to a rapid change in the background wind speed and direction. Ri profile on 6 December and 18 December 2005 (not shown) indicate higher stability in the upper troposphere region. Regions with low Ri decreased in comparison to convective days.

3.4 Observation of changes in wind and temperature due to convection

In this section, we show temporal behavior of temperature and wind components, especially in the lower and upper troposphere caused by convection. Stability changes in different layers in the troposphere and lower stratosphere due to vertical growth of convection and strong wind shears. Therefore during convection, at some heights a considerable change is seen in the temperature and wind fields.

Figure 5a–d shows time series of temperature (top panel), zonal wind (middle panel) and meridional wind (bottom panel) on 30 November, 6 December, 9 December and 18 December 2005. The time series is shown at 16 km height after removing their daily mean values. The diurnal components have also been removed from the wind and temperature to examine the effect of convection at a fine time scale in the lower and upper troposphere. Precautions have been taken primarily to observe the temperature changes caused solely by the convection and not as a result of diurnal variation.

From Fig. 5a and c (top panels), one can notice a decrease in temperature (~ 4 – 5 K) near 16 km height during active convection period on 30 November 2005 and 9 December 2005. An association of lower and upper troposphere through enhanced vertical motions may be inferred (see supplemental material, Fig. A3). Hourly data enabled us to delineate such fine time scale features. The cooling at ~ 16 km heights may have association with upward motions during active convection. Dhaka et al. (2001, 2005, 2006) had shown using VHF radars, that large vertical winds were usually accompanied with convection. In addition, humidity also enhanced with vertical winds, which penetrated into UTLS region after initiation of convection on both the convection days. Detail is shown in Sect. 3.7. Convection occurred much intense and deep on 9 December 2005, as the temperature dropped at ~ 15 – 16 km height even below CPT value during convection.

The mechanism of decreasing temperature is quite complex. The rate of decrease in temperature near the top of the cloud is fast. Satellite data also supports (cloud top brightness temperature values lies in the range ~ -60 °C to -70 °C) that the height of cloud top lies at the level of 14–15 km height, where the temperature decreased at most.

We take this opportunity to determine changes in temperature and wind in the lower troposphere and upper troposphere simultaneously. On both days of convection, fall in temperature, just below tropopause region, was accompanied by a significant change in speed and direction of zonal and meridional wind (Fig. 5a, c, middle and lower panels). For instance, change in speed and direction in zonal and meridional wind was observed by 10 – 12 m s $^{-1}$ during convection. Winds became significantly modified over a period of active convection (5–6 h). Such features were not evident on non-convective days (see Fig. 5b, d). Decrease in the temperature in the upper troposphere was observed within 1 km depth (from 15.6 km to 16.9 km) on both the convection days, which is shown in Fig. 6. Temperature anomalies are plotted in Fig. 6. Time series analysis, in the tropopause region (around 16 km height) on both the convective days, shows that maximum decrease in temperature occurred during convection initiation and its subsequent vertical growth. By looking carefully at a fine time resolution, we could infer that the substantial change (large fluctuation) in temperature was observed at ~ 15.6 km height, which is located close to strong wind shear (Fig. 2b), thereby suggesting that wind

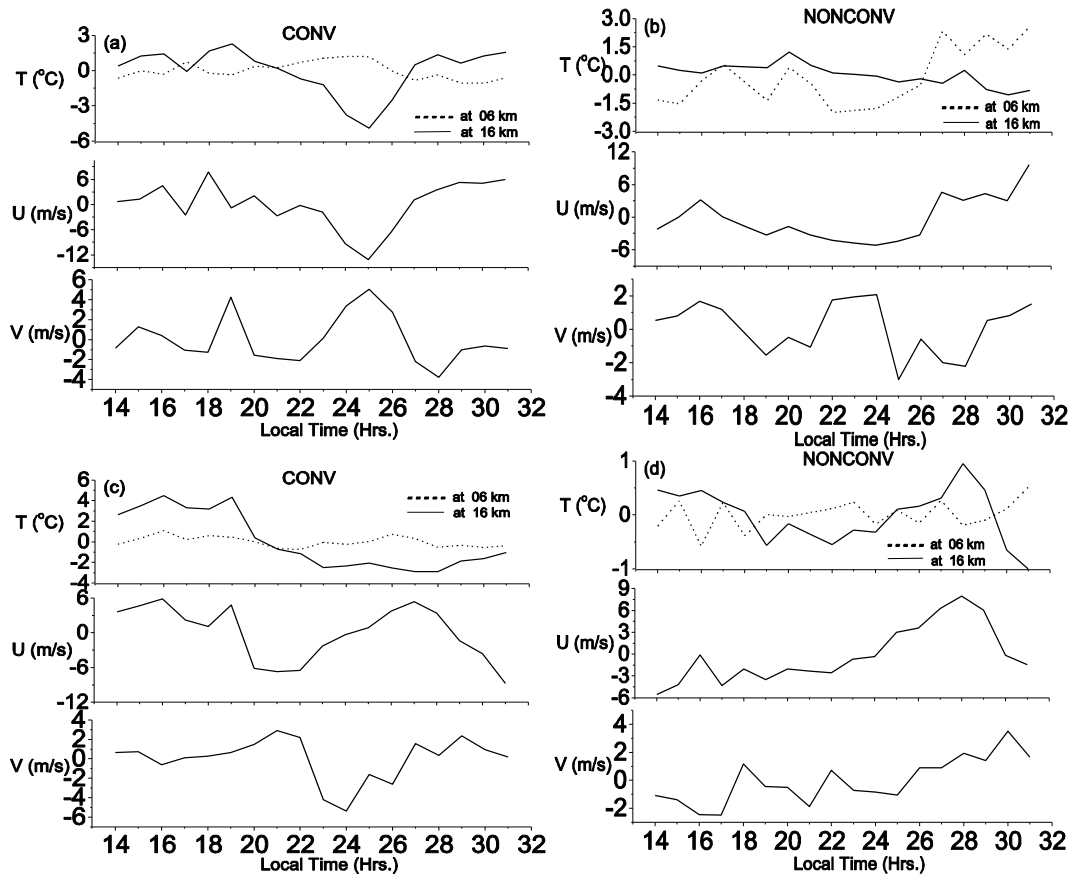


Fig. 5. Time series of the anomalies of temperature (upper panels), zonal wind (middle panels) and meridional wind (lower panels) are shown on (a) 30 November 2005, (b) 6 December 2005, (c) 9 December 2005, and (d) 18 December 2005. In the upper panels, dotted and solid line denotes variation in temperature at 6 km and 16 km height, respectively.

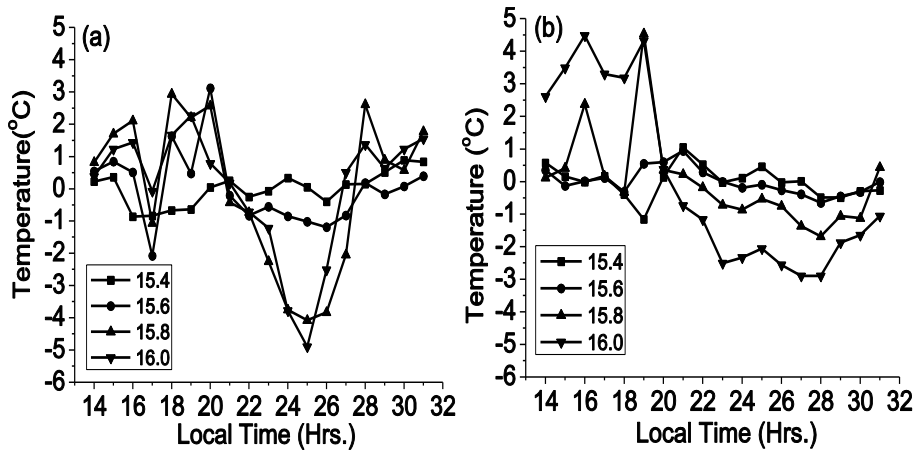


Fig. 6. Temporal variation of temperature in the upper troposphere (near tropopause region) from 15.4 km to 16.0 km height at 200 m height interval for convection days (a) on 30 November 2005, (b) on 9 December 2005. Here we have shown mean removed fluctuations.

shear is also a key component other than adiabatic cooling to cause the low temperature.

The decrease in temperature is found on the order of 4–5 K even after removal of diurnal cycle and mean (Fig. 6) on both the convection days. This strongly supports that such a

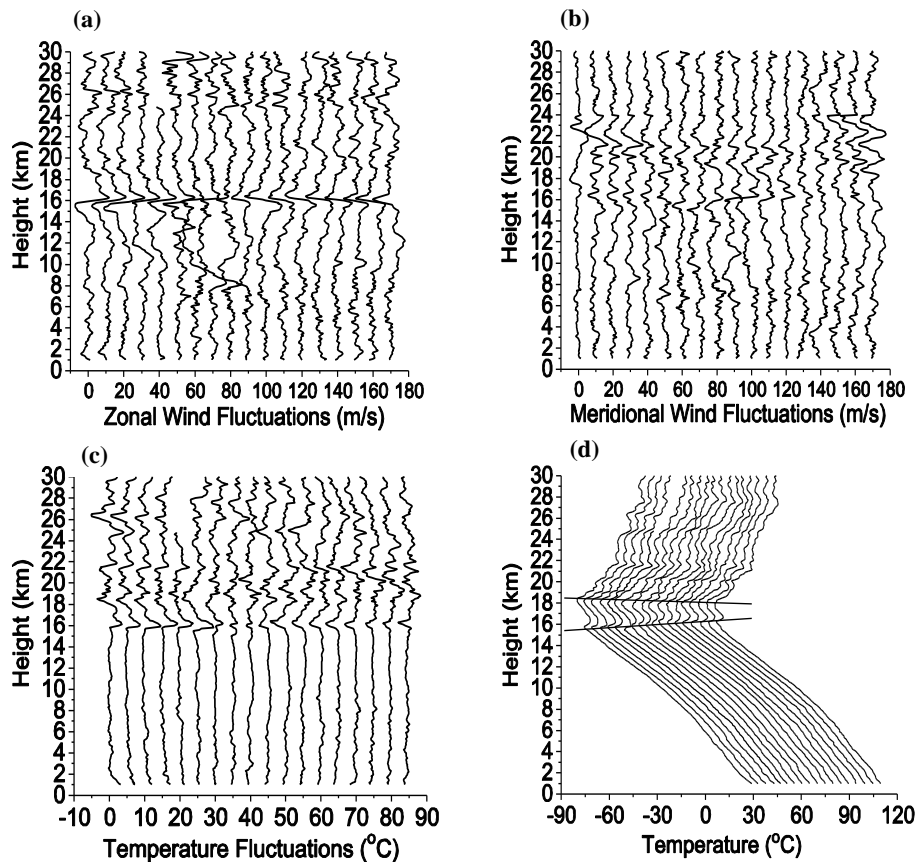


Fig. 7. Fluctuation in (a) zonal (upper panel left), (b) meridional wind (upper panel right), (c) temperature profiles (lower panel left), and (d) original temperature profiles (lower panel right) on 9 December 2005. Profiles are shown every hour starting at 13:00 LST to 07:00 LST (next day). These are shifted rightward by adding a constant (10 in upper panels and 5 in lower panels) to avoid overlapping. Two horizontal lines are drawn around 16 km and 18 km heights to denote the two tropopause height levels, which merges with time. Line drawn in meridional wind near 22 km shows a short vertical wavelength but long period waves (diurnal/semi diurnal).

sudden decrease in temperature is caused solely by convection and thus rejects the contribution of diurnal variation.

The amount of water vapor increases in the upper troposphere due to penetration of convection. This additional water content (in the form of ice particles in the upper troposphere) under the influence of strong wind shear seems to contribute to evaporation, leading to cooling. Also, the contribution is partly coming from radiative cooling and fast spread of air-mass (adiabatically) due to strong wind shear.

3.5 Fluctuation profiles of wind and temperature in the 1–30 km height range

Figure 7a–c shows fluctuations in zonal wind, meridional wind, and temperature profiles on 9 December 2005 – a convection day. Similar characteristic features were noted on the other convection day too (figure not shown). Wind and temperature fluctuations are shown in the range of 1–30 km height. Wave fluctuations showed some intriguing behavior near tropopause region.

One of the objectives of the analysis is to examine the fluctuations in the wind and temperature and also to determine their upward propagation/dissipation under varying wind speed. Therefore, mean wind and temperature profiles were subtracted from the individual profiles to extract the fluctuations. Mean wind and temperature profiles are shown earlier in Sect. 3.2 (Fig. 2) in the range of 1–30 km height.

Clear signatures of wave perturbations in temperature and zonal wind were identified above 16 km height. One can notice that near 16 km height (corresponds to WS1) a kind of phase reversal is seen (Fig. 7a–c) in the perturbations during convective occurrence on 9 December 2005. Such phase change is prominently seen caused by convection. Similar behavior was seen on 30 November 2005 (figure not shown). Such clear signatures and phase reversal patterns were not seen as prominently in non-convection days.

Hence, convection-induced patterns are unique in the tropopause region. Now, at higher heights (20 km and 25 km), a region between WS2 and WS3, the enhancement in perturbations were quite common on all days; as a result, we

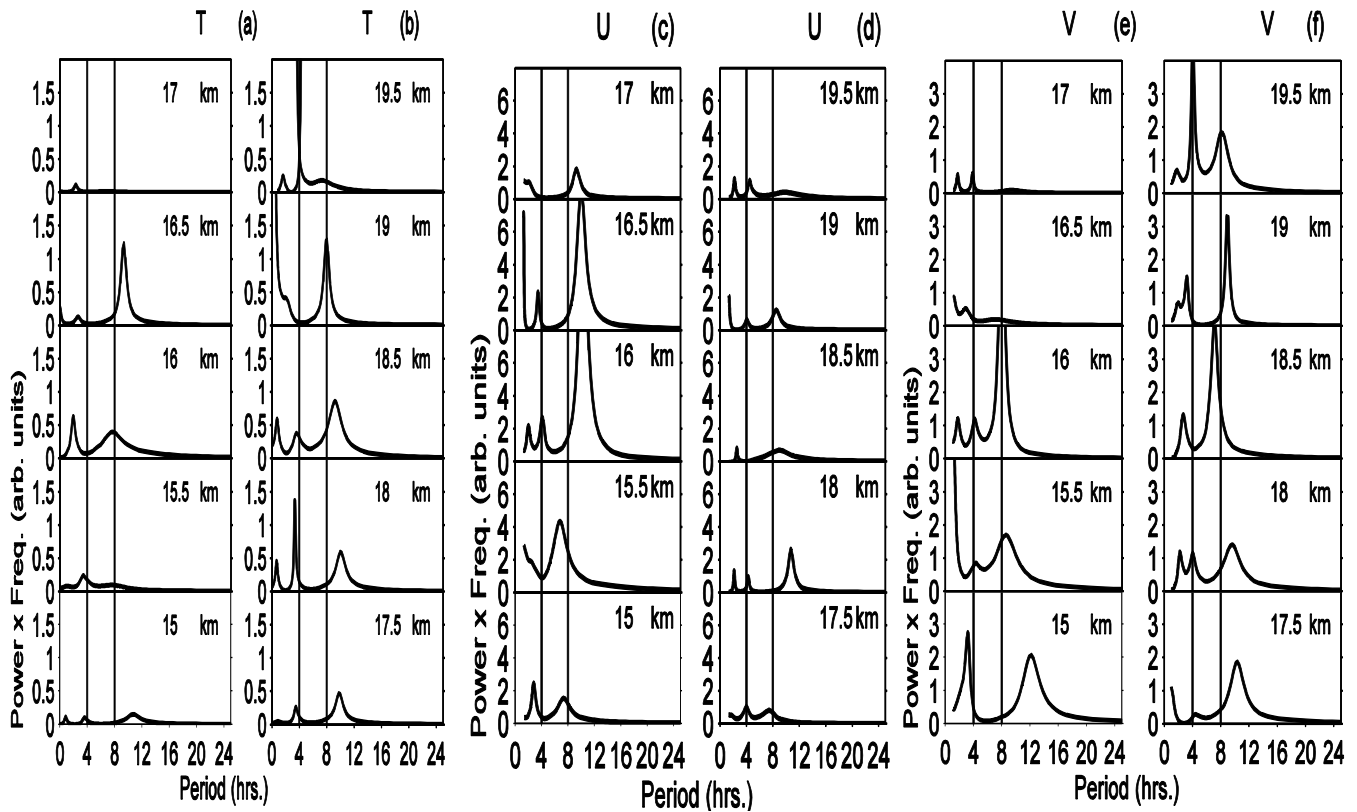


Fig. 8. From the spectrum of U , V , and T , we can infer dominant wave periods on 30 November 2005 at different height regions (from 15 to 19.5 km, at an interval of 0.5 km, mentioned in each plot) covering regions of WS1, tropopause, and WS2. Panels from left to right are shown for T (panels **a**, **b**), U (panels **c**, **d**), and V (panels **e**, **f**). Vertical lines are drawn on x-axis at 4 h and 8 h, respectively.

could not infer any clear distinction in the wave patterns at these heights, which could be due to convection occurrence. Figure 7d shows hourly temperature profiles. Some gradual changes in the thermal structure near tropopause are noted using hourly profiles. We carefully examined the lowest temperature peaks in the profiles near 16 and 18 km heights, which showed almost similar temperature values.

It appears that there are two tropopause levels. Recently, multiple tropopause have been reported in the equatorial region by Mehta et al. (2010), in Tibetan Plateau by Chen et al. (2011), and earlier by Yamanaka (1992). Mehta et al. (2010) have mentioned that the occurrence is more of multiple tropopause in the equatorial region. In this case, by sticking to a single peak over a period of several hours, one can see that the heights of the minimum temperature peaks (at 18 km and 16 km height) gradually become closer. The peak that appeared first at 18 km was decreased by about 0.5 km, and that of the 16 km height peak increased by about 1 km. Therefore, the two peaks seem to merge over a period of 15 h (from 13 h to 28 h, LST). Two solid lines are shown in Fig. 7d, which connect the lowest temperature peaks with time.

Similar patterns are noted on other days of observations, irrespective of convective and non-convective events. These contributed some evidence, showing daily variation in the height of CPT (by ~ 0.5 km) using hourly radiosonde data. High temporal resolution data enabled us to examine such interesting behavior. In the next section we show wave characteristics with periods less than 12 h by making use of hourly data.

3.6 Characteristics of wave systems

3.6.1 Wave periods

In order to characterize short period GWs (2–10 h in UTLS region), we applied a high pass filter with cutoff at 12 h to remove the diurnal cycle from temperature and wind time series at each 100 m interval. Dominant periods were computed in the troposphere and lower stratosphere region using MEM. Four interesting height regions are focused upon: (a) at first wind shear (WS1 – westward), which exists at ~ 16 km height; (b) at CPT (~ 17 –18 km); (c) at second wind shear (WS2 – eastward) i.e. ~ 20 km height; and at (d) third wind shear (WS3 – westward), which is located at ~ 25 km height. Analysis is performed during convective and non-convective

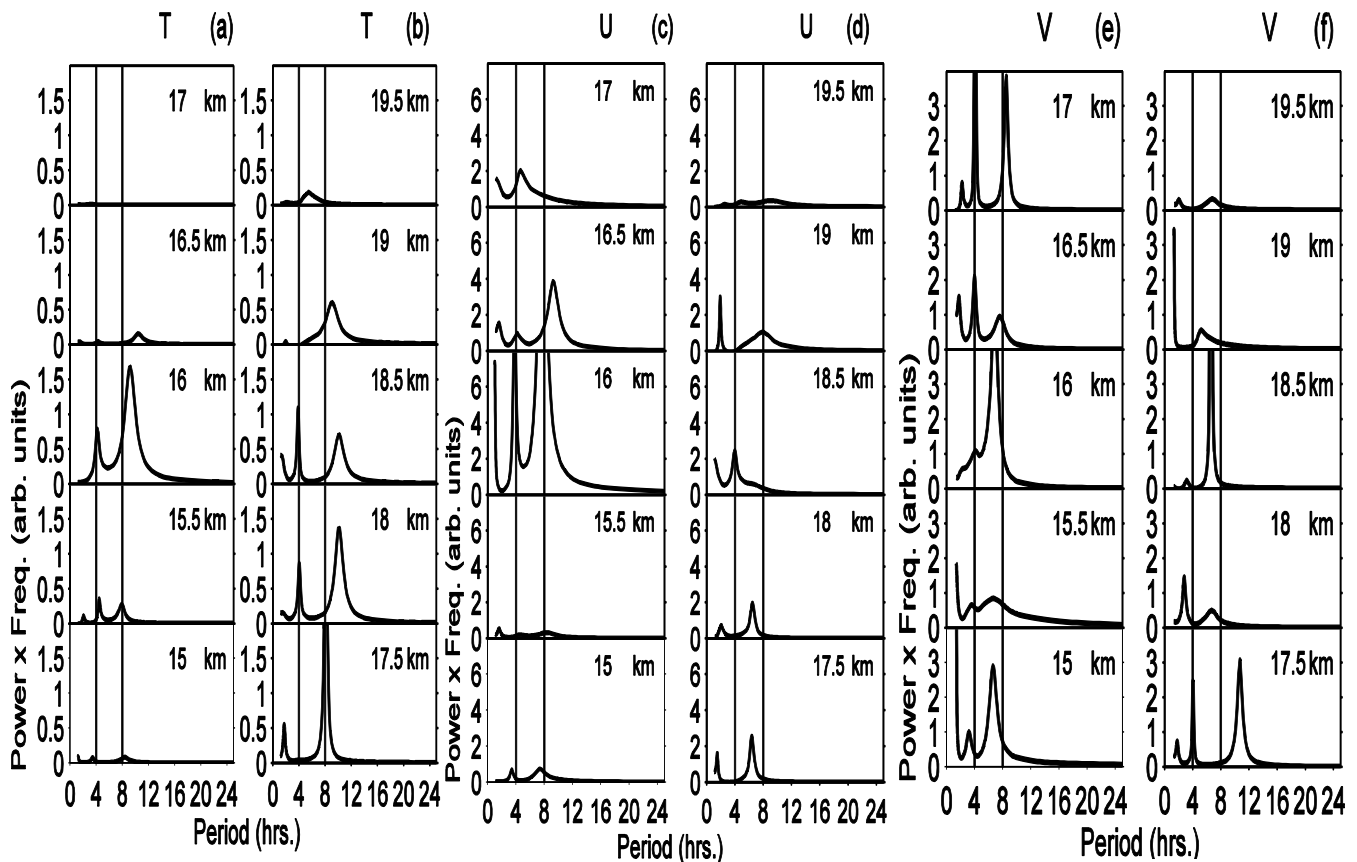


Fig. 9. Same as Fig. 8, but for 9 December 2005.

periods to examine the difference in the dominant wave characteristics.

As the stability and wind shear varied significantly with height in the upper troposphere and lower stratosphere, dominant wave periods of the emerged waves also changed with height. We examined different height regions at 100 m intervals (shown here at 500 m interval to avoid the crowded patterns) in order to examine the forcing scale in the frequency spectra due to convective and wind shear sources.

At WS1, dominant periods of about 4 and 10 h in T and U , and ~ 7 –8 h in V component are found on convective days (shown in Figs. 8 and 9, and Table 2). Note that strong wind shear on 30 November 2005 and 9 December 2005 were noted on the order of 45.7 and $58.6 \text{ m s}^{-1} \text{ km}^{-1}$, respectively. Above WS1, i.e. near tropopause, atmospheric stability increased substantially.

The CPT was located at $\sim 17.3 \text{ km}$ on both convective days. We noticed a strong wave with period ~ 8 –10 h present in temperature and wind field. This wave seems present at levels corresponding to WS1 and CPT on all 4 days of observation, irrespective of convection and no-convection.

Between tropopause and WS2, dominant short period GWs (~ 3 –4 h) emerged on 30 November 2005, while wave with periods $\sim 2 \text{ h}$ dominated on 9 December 2005. Such

slight difference in the emerged short wave periods on convection days might depend upon the penetrative depth of the convection, as on 9 December 2005 convection was intense and deeper than on 30 November 2005. At heights of WS2 and above, spectral power for the prominent wave periods reduced considerably. Note that mean wind between CPT and WS2 reduced from -35 m s^{-1} to $\sim 0 \text{ m s}^{-1}$. Similarly, dominant wave periods in this height region were also seen reduced from $\sim 10 \text{ h}$ and $\sim 4 \text{ h}$ to $\sim 7 \text{ h}$ and $\sim 2 \text{ h}$, respectively. This kind of feature in dominant wave periods denotes the wave filtering due to variation in background wind. Presence of short period waves ($\sim 2 \text{ h}$ on 9 December, and ~ 3 –4 h on 30 November 2005) are due to convection-induced gravity waves. During non-convection, wave periods were seen relatively enhanced.

At $\sim 25 \text{ km}$ height – a region of strong westward WS3 – the convection effect is less apparent on temperature and wind field. The observed characteristic features at this height region are in good agreement on all days. Similar short period (2–4 h) waves were present on all days. These short wave periods were associated with short vertical wavelength in the close vicinity of WS3.

Between 20 km and 30 km height, the ambient atmospheric conditions were different in comparison to middle

Table 2. Dominant wave periods in temperature (T) and wind components (both U and V) at CPT, WS1, WS2, and at WS3 along with information on wind shear and tropopause. The computed values of wave periods are rounded off to the nearest integer. Different periods in the UTLS region are the manifestation of change in stability and presence of strong wind shear.

Date & wave period	At CPT		Shear I		Shear II		Shear III	
	Height (km)	Value (°C)	Height (km)	Value (m s ⁻¹ km ⁻¹)	Height (km)	Value (m s ⁻¹ km ⁻¹)	Height (km)	Value (m s ⁻¹ km ⁻¹)
30 Nov 2005 (CONV) Wave period	17.2	-84.5	16.0	45.7	18.0	32.0	24.7	54.3
T	8, 3		10, 4		10, 4		9, 4	
U	6, 2		10, 4		7, 2		10, 4	
V	10, 4, 2		7		8		8	
9 Dec 2005 (CONV) Wave period	17.5	-85.1	16.2	58.6	19.3	28.2	24.6	44.6
T	10, 4-5		10		8, 3		4, 2	
U	10, 4, 2		10, 4		8, 4		8, 4	
V	10, 4, 2		8		8, 2		7, 2	
6 Dec 2005 (No Conv) Wave period	17.4	-82.2	16.3	47.7	19.7	-42.0	24.8	46.0
T	9, 5, 4		9, 2		10, 4		5, 2	
U	4		5		6-7		6, 4, 3	
V	4		6, 2		11, 4, 3		5, 3	
18 Dec 2005 (No Conv) Wave period	17.8	-83.8	15.1	44.8	19.3	30.0	24.4	58.3
T	7		8, 5, 2		12, 3		9, 3	
U	2		8, 4		7, 2		10, 2	
V	7, 3		8		3		10, 3	

and upper troposphere; hence, some features of GWs in this region seem different from those observed in the UTLS region. We examined the effect of convection in the 20–30 km height range in the presence of WS3 and noticed that short period waves are not influenced by convection, but rather they are generated near WS3 (Hodograph shown in Fig. 12).

3.6.2 Vertical wavelength

In order to examine the forcing scale in the vertical direction, we computed vertical wavelength in temperature and wind field during the observation period. Differences in λ_z during convection and non-convection enabled us to decipher the effect of convection growth in the troposphere and lower stratosphere. We focused on short scale (<12 h) wave features that emerged during convection. The mean temperature and wind (mean profiles were constructed using several profiles covering about a week period) were subtracted from the individual profiles to retain the dominant fluctuations. We computed λ_z using profiles of anomalies from hourly radiosonde by MEM power spectrum analysis. Computed λ_z is shown sequentially in Fig. 10 (30 November 2005) and Fig. 11 (9 December 2005) for temperature and U , V wind components between 16 and 30 km heights. Between 1

and 16 km heights, spectra for vertical wavelengths are also plotted. These power spectra are named as “source” spectra, which show the characteristics of tropospheric convective sources; while between 16 km and 30 km heights, the spectra are named as “gravity wave (GW)” spectra. In all the panels, time sequence is marked in each plot that increases upwards from the bottom. Power spectra for temperature, U and V wind are shown in Figs. 10–11 (panels a, b; panels c, d; and panels e, f), respectively.

On 30 November and 9 December 2005, before setting up of convection, λ_z in temperature, U and V wind components were observed ~ 3 –5 km with maximum power shared in 4–5 km range. During convection, peaks ~ 1 –2 km emerged gradually along with weakening of primary peak of 3–4 km in temperature, U , and V components, showing the influence of convection. Over a certain period during convection growth, spectral power remains comparable for both short (~ 2 km) and long (~ 3 –5 km) vertical wavelengths. Note the fact that vertical wavelength is not conserved along a ray path in a refractive atmosphere, but rather it changes in a given height range (see auxiliary material, Fig. A4). Computed values of vertical wavelength, therefore, show an average feature.

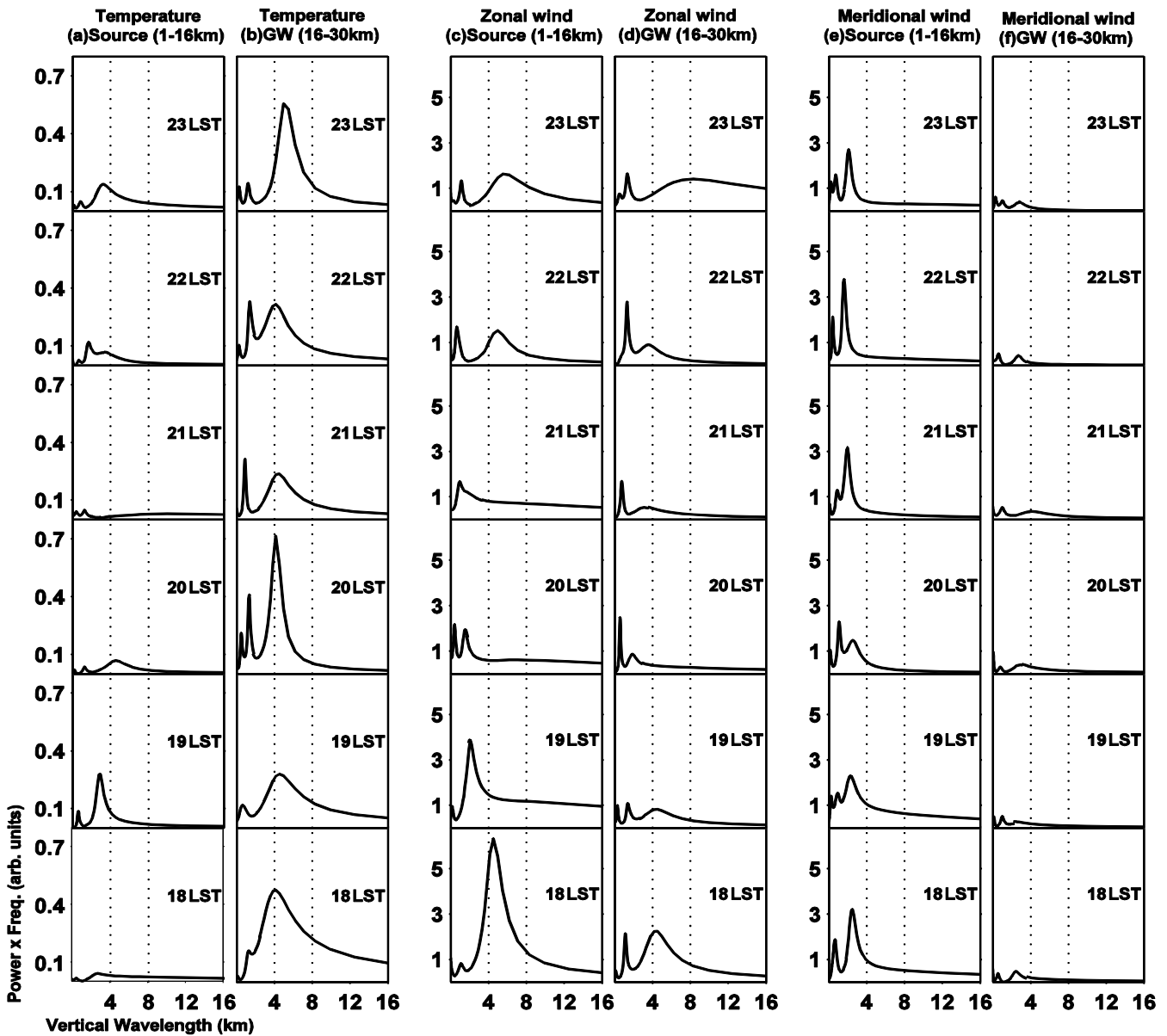


Fig. 10. Temporal distribution of Vertical wavelength (λ_Z) for temperature (panels a, b), zonal wind (panels c, d) and meridional wind (panels e, f) on 30 November 2005. Panels (a), (c), and (d) denote source power spectra (1–16 km heights), while panels (b), (d), and (f) denote GW spectra as they are computed between 16 and 30 km height range. Source spectra were multiplied by a factor of “3” to increase the power for comparison with GW. The panels are arranged columnwise. Vertical lines drawn on x-axis denote vertical wavelength at 4 km and 8 km, respectively. Y-axis represents power (in arbitrary units) in all panels.

Spectral peaks with ~ 2 km that emerged as a result of convection dissipate with time. After termination of convection, λ_Z in T , U and V components increased (~ 3 – 5 km), approaching the similar wavelength that was observed before convection. Penetration of convection in UTLS and the resulting forcing scale is clearly visible in temperature and wind field over the active period of convection.

Convection-induced wave behavior noticed on the vertical wavelength distribution suggests that increased power near short vertical wavelength (~ 2 km) is contributed to by convective system. On 30 November and 9 December 2005, GW spectra are more prominent than source spectra in temperature. Both source spectra and GW spectra are similar in zonal and meridional wind, except on 9 December when source spectra is broader in zonal wind for the active convection period. There is no clean signature of half sine wave

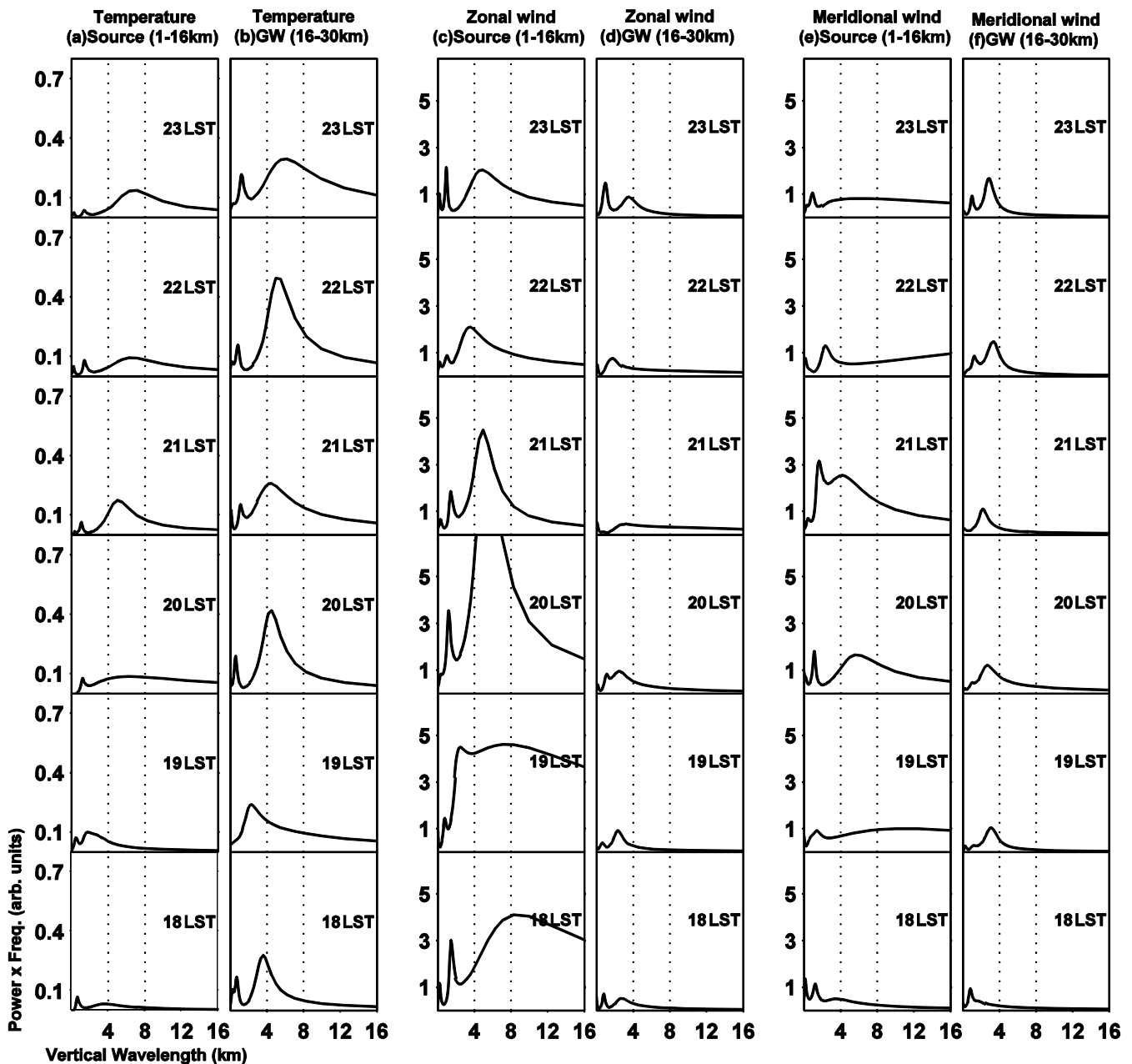


Fig. 11. Same as that for Fig. 10 but for 9 December 2005.

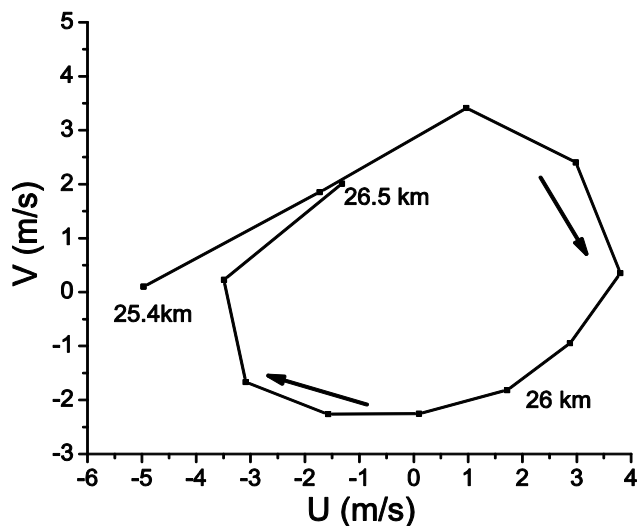
response of vertical wavelength from the troposphere to the lower stratosphere matching with the mechanism of thermal heating and its response in terms of vertical forcing.

During non-convective days (6 December and 18 December), in general, T , U and V components showed that main peaks of vertical wavelength remain around 3–5 km. Note that on 7 December (morning hours 3–5 a.m.), a convective patch over a duration of about 3–4 h appeared at ~ 8 km altitude. The immediate response of the convection patch was observed to reduce the λ_z (down to ~ 2 km) in a similar manner as observed for convection days. On 18 December 2005,

we did not notice the gradual change in the vertical wavelength as observed on early morning of 7 December (not shown). In general, the V component showed less vertical wavelength in comparison to U component and temperature. Details of dominant peaks on different days are shown in Table 3. A comparison of peaks before, during and after convection can also be inferred. In the last column, we have included wavelengths, which were computed after termination of convection (not shown in Figs. 10 and 11). Figure 12 shows hodograph formed using U wind and V wind components at heights which are just above the WS3. Short vertical

Table 3. Dominant vertical wavelengths in temperature, U and V wind components are shown.

Date	Parameter	λ_z (before convection)	λ_z (during convection)	λ_z (after convection)
30 Nov 2005 (Convection)	Temperature	3	1, 2, 4	2, 5
	U Comp	4	1, 2, 4	2, 5
	V Comp	2	1, 2	3, 4
9 Dec 2005 (Convection)	Temperature	2, 3, 4	1, 2, 3	1, 5, 6
	U Comp	1, 4, 5	1, 2	3, 4
	V Comp	2, 3	1, 2	3, 5

**Fig. 12.** Hodograph between 25.4 km and 26.5 km height on 30 November 2005. Hodograph ellipse completed within ~ 1 km height.

wavelength (~ 1 km) gravity waves are generated in the close vicinity of WS3. A similar feature was observed between temperature and U wind component in the same height region.

As shown in Fig. 2, a strong WS3 exists near 25 km height (see Table 1 for magnitudes on different days). We have also analyzed temperature and U wind hodograph showing similar structure as seen in Fig. 12. This suggests that a well-defined wave pattern is generated due to strong wind shear. This is also confirmed by examining each temperature and wind profile on all days near 25 km height. Since such small scale hodographs emerged on both convective and non-convective days, convection does not therefore seem to be the source. One can infer from such structures that waves with small vertical wavelengths are consistently present at this height region and produced by wind shear.

3.7 Relationship of humidity with vertical wind (W) and temperature

As mentioned earlier, humidity was enhanced with large fluctuations during active convection in the UTLS region on both days of convection (30 November and 9 December 2005). As a result, the quasi-periodic behavior of humidity and temperature became prominent in this region. Association of humidity rise with vertical wind (Figs. 13 and 14) confirms the vertical growth of convection. We examined the correlation of humidity and W component over a period of active convection in the UTLS. It is evident from Figs. 13 and 14 that both the parameters are well correlated. The rise in humidity is associated with upward W wind even at the heights above tropopause. Note that around 18:00 LST, there is a sharp increase in the humidity along with rise in upward motions that continued over a period of active convective (see supplement for vertical wind – Fig. A3). With the passage of time, decrease in humidity and W component is commonly seen.

The mechanism of temperature control before and during convection could be different in the upper troposphere because of the change in the humidity content after setting up of the convection. Strong (weak) R_{xy} (between humidity and temperature) on convection (non-convection) days indicates that significant increase in humidity in a quasi-periodic way during convection plays a crucial role in inducing small-scale oscillations in temperature and wind in the UTLS region. It appears that variation in humidity is in association with variation in vertical growth in convective system (and hence vertical wind), which eventually can produce similar patterns in temperature. There is a possibility that increase in humidity lead to small-scale oscillations in flow field via turbulence and mixing.

In order to assess the effect of penetration of convection into the UTLS region, variance of temperature and humidity were also computed at different height levels to see the relative enhancement for both convection dates (30 November and 9 December 2005); the variances were larger in the height range of 16 km to 19 km. For instance, on the convection days the humidity variance noted was as large as 200 at 18.3 km on 30 November 2005 and ~ 227 at 16.7 km on 9 December 2005. The value of temperature variance, found to be

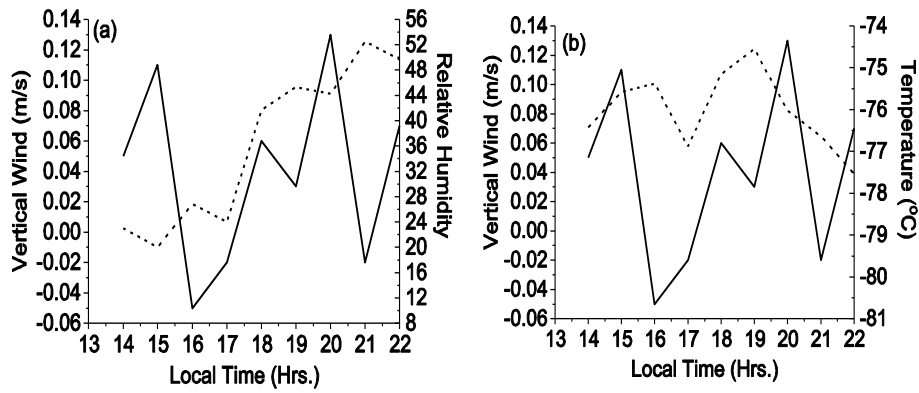


Fig. 13. (a) Temporal behavior of humidity (dotted line) and vertical wind (solid line), (b) Temporal behavior of temperature (dotted line) and vertical wind (solid line) in the UTLS region (16 km height) on 30 November 2005.

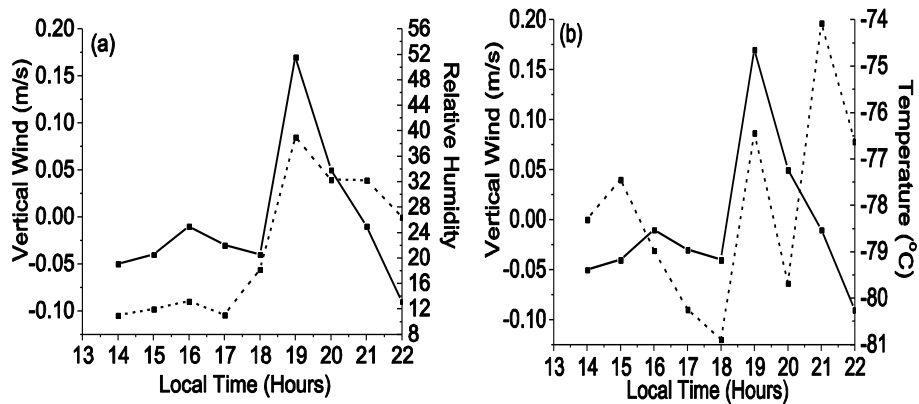


Fig. 14. (a) Temporal behavior of humidity (dotted line) and vertical wind (solid line), (b) temporal behavior of temperature (dotted line) and vertical wind (solid line) in the lower stratosphere (19 km height) on 9 December 2005.

4 on 30 November vs. 9.8 on 9 December 2005, indicates a deeper and stronger convective event on 9 December 2005. For both the non-convective days, the humidity and temperature variance was 3–9 times smaller as compared to that for convection days. This suggests that such large variances in temperature and humidity in the case of convection days are a consequence of deep penetration of the convection into the UTLS region.

4 Summary and concluding remarks

In this paper, an attempt has been made to present the general characteristics of the emerged wave system in terms of vertical wavelengths and prominent wave frequencies, and the vertical structure of the convective system during an intensive observation period, by launching hourly radiosonde and radars data under CPEA-II campaign. As one of the objectives of this paper was to carefully examine the wave disturbances on a time scale of less than semi-diurnal oscillations, wind and temperature data were therefore high-pass

filtered with a cutoff at 12 h. The results are shown in terms of dominant wave frequencies at different height levels under varying basic wind in the height range of 1–30 km.

Mean wind and temperature profiles showed that there were three different height regions of strong wind shear: the lowest one was around 16 km height ($\sim 49.2 \text{ m s}^{-1} \text{ km}^{-1}$), the middle one at $\sim 20 \text{ km}$ ($\sim 33.0 \text{ m s}^{-1} \text{ km}^{-1}$), and the upper one was located at $\sim 25 \text{ km}$ height ($\sim 50.6 \text{ m s}^{-1} \text{ km}^{-1}$). Thin layers of low Ri were confined near these wind shears. In addition, less stable region with low Ri (< 0.25) was observed during convective storm penetration in the 12–16 km height, which was more prone to instability due to the presence of cloud system. Hourly temperature measurement near 16 km height (level of the top of the cloud and strong wind shear) showed a significant decrease in temperature on the order of $\sim 4\text{--}5 \text{ K}$ during convection. Decrease in temperature persisted over a duration of active convection, and the recovery in temperature to its mean value was also seen after the termination of convection. During vertical growth of convection, wind speed and direction also changed drastically, causing small scale wave generation in the UTLS region.

Signatures of decrease in temperature at tropopause level and their seemingly association with the rise in temperature at ~ 6 km height (on 30 November 2005) suggests vertical growth of convection system adiabatically.

The cause of the decrease in temperature, confined in thin layer near 16 km height (note that cold point temperature observed at ~ 17.3 km height) during active convection, is believed to be mainly mechanized by strong wind shear and partly by the adiabatic expansion of air-mass from the lower troposphere to the upper troposphere. As mentioned in Sect. 3.4, decrease in temperature is confined in a thin layer of ~ 1 km in the close vicinity of wind shear and top of the cloud (humidity at those levels also increased); therefore, evaporation appears to be the more effective cooling process. Hourly observation of temperature enabled us to confirm such phenomena on both days of convection. Increase in humidity in the troposphere and extending up to 19 km height was also recorded during convection days, which is larger by a factor of 2–3 in comparison to non-convection days. Quasi-periodic variations in temperature and humidity were found anti-correlated more strongly than in non-convective days, suggesting that increase in humidity locally can lead to decrease in temperature in the presence of strong winds. Humidity in the stratosphere-troposphere exchange process has been identified to play a significant role.

Signature of distinct wave system is identified in the upper troposphere and lower stratosphere. Therefore, filtering of GWs took place due to presence of wind shear. For instance, waves with ~ 10 h and 4 h periods were dominant near 16 km height, which were present on all days of observation irrespective of convection or non-convection times. Between 17 km and 20 km heights, wave-like signatures were dominant in meridional wind and temperature, and also convection-induced waves with periods ~ 2 h were noticed in temperature, humidity and wind.

However, at heights between 21 and 30 km, GWs with periods in the range of 2–3 h, 4–5 h and ~ 8 –10 h were seen in zonal wind and temperatures. Variation in dominant wave periods with height is associated with changing wind speed.

Figures 13 and 14 show that T and W components are well associated in the 16–20 km height region, which suggests vertical orientation of the generated wave system. The vertical motions also became enhanced in the tropopause region (16–18 km height) during convection; as a result, the average vertical wind remained positive (~ 0.5 m s $^{-1}$). However, a hodograph formed (not shown) between 17 and 20 km height by horizontal wind components showed a complex behavior of clockwise and anti-clockwise rotation, denoting mixture of downward and upward energy propagation. The closing of the hodograph covered ~ 1 –2 km height, suggesting further that short vertical wavelength dominated during convection. Hodograph behavior between 17 and 20 km height suggests that secondary sources are also important to generate such small scale features. Importance of secondary sources has been addressed by Holton and Alexander (1999), Walter-

scheid and Sivjee (2001); Horinouchi et al. (2002); Snively and Pasko (2005); and Chun and Kim (2008). They also have discussed waves, especially with small vertical wavelengths during convective period that are likely related to the secondary sources.

Computations of average λ_z were also performed using wind and temperature fluctuations profiles in the 16–30 km height range. In general, zonal, meridional, and temperature profiles showed that vertical wavelength in the range 2–5 km is quite dominant. A clear variation in λ_z during convection and non-convection is also identified: short vertical wavelength (~ 1 –2 km) dominated during convection and the power of spectra also increased by a factor of 2–3. This suggests that a large spectrum of wave with short λ_z generates invariably in this region, though their vertical propagation could not be sustained due to fast dissipation in the presence of strong wind shear. Therefore, after termination of convection, waves with vertical wavelength ~ 3 –5 km were present.

Some unique features at ~ 25 km height, a level of strong wind shear, were also noticed: short period waves (~ 2 –4 h) were generated with short λ_z (~ 1 –1.5 km) and were highly confined near wind shear, suggesting this to be a source region for such variations and not related with convection in the troposphere. Zonal wind and temperature perturbations near 25 km showed a closed hodograph in the form of ellipse, suggesting east-west propagation of short λ_z GWs generated due to strong wind shear (Fig. 12). We have shown a sample for the generation of the short period gravity waves on 30 November 2005.

During active convection, upward motion enhanced and the relative humidity also increased in the UTLS region. The relationship of humidity and vertical wind is analyzed and shown well correlated during convection at a fine time resolution; therefore, the current observations also provide valuable information on this aspect.

Supplementary material related to this article is available online at:

<http://www.ann-geophys.net/29/2259/2011/angeo-29-2259-2011-supplement.pdf>

Acknowledgements. The work is supported by RESPOND – ISRO. Authors are thankful to the CPEA-II team for providing radiosonde data. The EAR is operated by Research Institute for Sustainable Humanosphere (RISH) of the Kyoto University, Japan, and the Indonesian National Institute of Aeronautics and Space (LAPAN). S. K. Dhaka acknowledges the support of JSPS as part of the work was performed during his visit to Kyoto University, Japan.

Topical Editor C. Jacobi thanks three anonymous referees for their help in evaluating this paper.

References

- Abraham, S., Dhaka, S. K., Preveen, K. D., Nath, N., Nagpal, O. P., and Baluja, K. L.: Planetary wave effect on ionosphere absorption, *J. Atmos. Solar Terr. Phys.*, 60, 441–453, 1998.
- Alexander, M. J., Holton, J. R., and Durran, D. R.: The gravity wave response above deep convection in a squall line simulation, *J. Atmos. Sci.*, 52, 2212–2226, 1995.
- Alexander, S. P., Tsuda, T., Furumoto, J., Shimomai, T., Kozu, T., and Kawashima, M.: A statistical overview of convection during the First CPEA Campaign, *J. Meteor. Soc. Japan*, 84A, 57–93, 2006.
- Alexander, S. P., Tsuda, T., Shibagaki, Y., and Kozu, T.: Seasonal gravity wave activity observed with the Equatorial Atmosphere Radar and its relation to rainfall information from the Tropical Rainfall Measuring Mission, *J. Geophys. Res.*, 113, D02104, doi:10.1029/2007JD008777, 2008.
- Barrodale, I. and Erikson, R. E.: Algorithms for least squares linear prediction and maximum entropy method. Part I – Theory, *Geophys.*, 40, 420–446, 1980.
- Chen, X. L., Ma, Y. M., Kelder, H., Su, Z., and Yang, K.: On the behaviour of the tropopause folding events over the Tibetan Plateau, *Atmos. Chem. Phys.*, 11, 5113–5122, doi:10.5194/acp-11-5113-2011, 2011.
- Chun, H.-Y. and Kim, Y.-H.: Secondary waves generated by breaking of convective gravity waves in the mesosphere and their influence in the wave momentum flux, *J. Geophys. Res.*, 113, D23107, doi:10.1029/2008JD009792, 2008.
- Chun, H.-Y., Song, I.-S., Baik, J.-J., and Kim, Y.-J.: Impact of a convectively forced gravity wave drag parameterization in NCAR CCM3, *J. Climate.*, 17, 3530–3547, 2004.
- Dhaka, S. K., Devrajan, P. K., Shibagaki, Y., Choudhary, R. K., and Fukao, S.: Indian MST radar observations of gravity wave activities associated with tropical convection, *J. Atmos. Solar-Terr. Phys.*, 63, 1631–1642, 2001.
- Dhaka, S. K., Yamamoto, M. K., Shibagaki, Y., Hashiguchi, H., Yamamoto, M., and Fukao, S.: Convection-induced gravity waves observed by the Equatorial Atmosphere Radar [0.200 S, 100.320 E] in Indonesia, *Geophys. Res. Lett.*, 32, L14820, doi:10.1029/2005GL022907, 2005.
- Dhaka, S. K., Yamamoto, M. K., Shibagaki, Y., Hashiguchi, H., Fukao, S., and Chun, H.-Y.: Equatorial Atmosphere Radar observations of short vertical wavelength gravity waves in the upper troposphere and lower stratosphere region induced by localized convection, *Geophys. Res. Lett.*, 33, L19805, doi:10.1029/2006GL027026, 2006.
- Dhaka, S. K., Bhatnagar, R., Shibagaki, Y., Fukao, S., Kozu, T., Malik, V., Malik, S., and Dutta, A.: Study of temporal variation of equatorial tropopause due to atmospheric waves in CPEA Campaign 2004 at Koto Tabang, Indonesia, *Adv. Geosci.*, 11, 167–175, 2007a, <http://www.adv-geosci.net/11/167/2007/>.
- Dhaka, S. K., Yamamoto, M. K., Shibagaki, Y., Hashiguchi, H., Yamamoto, M., Kozu, T., Shimomai, T., and Fukao, S.: Observations of convection Events and generated high frequency gravity waves over Koto Tabang, Indonesia using Equatorial Atmosphere Radar [0.2 S, 100.3 E], in: *Proceedings of the INTAR*, edited by: Anandan, V. K., Roettger, J., and Narayan Rao, D., pp. 46–56, NARL, Department of Space, ISRO, 2007b.
- Fritts, D. C. and Alexander, M. J.: Gravity wave dynamics and effects in the middle atmosphere, *Rev. Geophys.*, 41, 1, doi:10.1029/2001RG000106, 2003.
- Fukao, S.: Coupling Processes in Equatorial Atmosphere [CPEA]: A project overview, *J. Meteor. Soc. Japan*, 84A, 1–18, 2006.
- Holton, J. R. and Alexander, M. J.: Gravity waves in the mesosphere generated by tropospheric convection, *Tellus*, 51A-B, 41–58, 1999.
- Horinouchi, T., Nakamura, T., and Kosaka, J.: Convectively generated mesoscale gravity waves simulated throughout the middle atmosphere, *Geophys. Res. Lett.*, 29, 2007–2010, doi:10.1029/2002GL016069, 2002.
- Lane, T. P., Reeder, M. J., and Clark, T. L.: Numerical modeling of gravity wave generation by deep tropical convection, *J. Atmos. Sci.*, 58, 1249–1274, 2001.
- Mehta, S. K., Ratnam, V., and Krishna Murthy, B. V.: Characteristics of multiple tropopauses in the tropics, 38th COSPAR Scientific Assembly, Held 18–15 July 2010, in Bremen, Germany, p. 4, 2010.
- Ratnam, M. V., Tetzlaff, G., and Jacobi, C.: Global and Seasonal Variation of Stratospheric GW activity deduced from the CHAMP/GPS satellite, *JAS*, 61, 1610–1620, 2004.
- Ratnam, M. V., Tsuda, T., Shibagaki, Y., Kozu, T., and Mori, S.: Gravity Wave Characteristics over the Equator Observed During the CPEA Campaign using Simultaneous Data from Multiple Stations, *J. Meteor. Soc. Japan*, 84A, 239–257, 2006.
- Schodel, J. P. and Munk, J. W.: Methods for investigation of the spectral frequency distribution of gravity waves in the ionosphere, *Z. Geophys.*, 38, 169, 1972.
- Shibagaki, Y., Kozu, T., Shimomai, T., Mori, S., Murata, F., Fujiyoshi, Y., Hashiguchi, H., and Fukao, S.: Evolution of a Super Cloud Cluster and the Associated Wind Field Observed over the Indonesian Maritime Continent during the First CPEA Campaign, *J. Meteor. Soc. Japan*, 84A, 19–31, 2006a.
- Shibagaki, Y., Shimomai, T., Kozu, T., Mori, S., Fujiyoshi, Y., Hashiguchi, H., Yamamoto, M. K., Fukao, S., and Yamanaka, M. D.: Multiscale aspects of convective systems associated with an intraseasonal oscillation over the Indonesian Maritime Continent, *Mon. Weather Rev.*, 134, 1682–1696, 2006b.
- Snively, J. B. and Pasko, V. P.: Antiphase OH and OI airglow emissions induced by a short-period ducted gravity wave, *Geophys. Res. Lett.*, 32, L08808, doi:10.1029/2004GL022221, 2005.
- Tsuda, T., Murayama, Y., Wiryosumarto, H., Harijono, S. W. B., and Kato, S.: Radiosonde observations of Equatorial Atmosphere Dynamics over Indonesia. 1. Equatorial Waves and Diurnal Tides, *J. Geophys. Res.*, 99, 491–505, 1994.
- Tsuda, T., Ratnam, V. M., Kozu, T., and Mori, S.: Characteristics of 10-day Kelvin Wave Observed with Radiosondes and CHAMP/GPS Occultation during the CPEA Campaign [April–May, 2004], *J. Meteor. Soc. Japan*, 84A, 277–293, 2006.
- Vincent, R. A. and Alexander, M. J.: Gravity waves in the tropical lower stratosphere: An observational study of seasonal and inter-annual variability, *J. Geophys. Res.*, 105, 17971–17982, 2000.
- Walterscheid, R. and Sivjee, G. G.: Zonally symmetric oscillations observed in the airglow from South Pole station, *J. Geophys. Res.*, 106, 3645–3654, 2001.
- Yamanaka, M. D.: Formation of multiple tropopause and stratospheric inertio-gravity waves, *Adv. Space Res.*, 12, 181–190, 1992.